AGU PUBLICATIONS

JGR

Journal of Geophysical Research: Space Physics

RESEARCH ARTICLE
10.1002/2015JA021493-T

Key Points:
- A new zonal drift velocity and tilt estimation method
- Detailed study on zonal drift velocity and tilt
- A finding that zonal drift velocity and tilt are correlated

Correspondence to:
S. Ji,
jidifferent@gmail.com

Citation:
Ji, S., W. Chen, D. Weng, and Z. Wang (2015), Characteristics of equatorial plasma bubble zonal drift velocity and tilt based on Hong Kong GPS CORS network: From 2001 to 2012, *J. Geophys. Res. Space Physics*, *120*, 7021–7029, doi:10.1002/2015JA021493-T.

Received 26 MAY 2015
Accepted 23 JUL 2015
Accepted article online 1 AUG 2015
Published online 26 AUG 2015

Characteristics of equatorial plasma bubble zonal drift velocity and tilt based on Hong Kong GPS CORS network: From 2001 to 2012

Shengyue Ji[1,2], Wu Chen[2], Duojie Weng[2], and Zhenjie Wang[1]

[1]School of Geosciences, China University of Petroleum (Huadong), Qingdao, China, [2]Department of Land Surveying and Geo-Informatics, Hong Kong Polytechnic University, Hung Hom, Hong Kong

Abstract Hong Kong (22.3°N, 114.2°E, dip: 30.5°N; geomagnetic 15.7°N, 173.4°W, declination: 2.7°W) is a low-latitude area, and the Hong Kong Continuously Operating Reference Station (CORS) network has been developed and maintained by Lands Department of Hong Kong government since 2001. Based on the collected GPS observations of a whole solar cycle from 2001 to 2012, a method is proposed to estimate the zonal drift velocity as well as the tilt of the observed plasma bubbles, and the estimated results are statistically analyzed. It is found that although the plasma bubbles are basically vertical within the equatorial plane, the tilt can be as big as more than 60° eastward or westward sometimes. And, the tilt and the zonal drift velocity are correlated. When the velocity is large, the tilt is also large generally. Another finding is that large velocity and tilt generally occur in spring and autumn and in solar active years.

1. Introduction

Plasma bubble is an important phenomena of equatorial ionosphere, and the ionospheric irregularities within the bubble can cause scintillation that can seriously disrupt the operation of nearly all space and ground-based systems that rely on trans-ionospheric propagation of radio frequencies [*Aarons*, 1993].

The study of equatorial ionospheric plasma drifts and tilts is an important part of the equatorial space science research and of fundamental importance for space weather monitoring and forecasting. A lot of research works on ionospheric plasma drift at the magnetic equator have been made with various instruments, including incoherent scatter radar [*Fejer*, 1981; *Fejer et al.*, 1991], the DE-2 satellite [*Aggson et al.*, 1987; *Coley and Heelis*, 1989; *Fejer et al.*, 1995], all-sky imager [*Mendillo and Baumgardner*, 1982; *Abdu et al.*, 1987; *Rohrbaugh et al.*, 1989; *Sobral and Abdu*, 1990, 1991; *Tinsley et al.*, 1997; *Pimenta et al.*, 2003; *Martinis et al.*, 2003], and GPS receivers [*Aarons et al.*, 1996; *Kelley et al.*, 1996; *Beach et al.*, 1997; *Musman et al.*, 1997; *Kil et al.*, 2000, 2002; *Kintner et al.*, 2001, 2004; *Makela et al.*, 2004; *Otsuka et al.*, 2006]. Past research found that the drift is generally in zonal direction and the velocity is generally between 50 m/s and 200 m/s. A bubble typically forms following sunset, drifts eastward, and the eastward drifting velocity decreases gradually, then turns to west steadily after midnight. A gradual decrease in the zonal drift velocity from between 100 and 200 m/s at around 22:00 LT to below 50 m/s after local midnight was reported [*Mendillo and Baumgardner*, 1982; *Mendillo et al.*, 1997; *Taylor et al.*, 1997; *Sinha and Raizada*, 2000; *Pimenta et al.*, 2003].

Although not as much research on tilt as on drift have been made, previous works show that the ionospheric bubbles are generally aligned from north to south along the magnetic field line. However, sometimes westward [*Mendillo and Tyler*, 1983; *Basu et al.*, 1996; *Abalde et al.*, 2001; *Kil et al.*, 2002; *Makela and Kelley*, 2003; *Mukherjee*, 2003; *Ogawa et al.*, 2005, 2006] or eastward [*Taylor et al.*, 2009; *Rohrbaugh et al.*, 1989] tilt can be observed. Most of times, the tilt is generally small, while sometimes it can reach up to as large as 47° [*Basu et al.*, 1996; *Makela and Kelley*, 2003; *Mukherjee*, 2003].

Most of these previous research works especially on tilt are case studies, such as for one geomagnetic storm or several days. The goal of this research is to make a detailed statistical study on both equatorial plasma drift and tilt from 2001 to 2012 based on the observations of Hong Kong GPS Continuously Operating Reference Station (CORS) of a whole solar cycle. Although similar research works had been done for the American longitudinal section [*Sobral et al.*, 1999], the present work is based on an extended data basis of plasma bubbles zonal drifts comprising 650 nights of experiments acquired during 12 years (1980–1992).

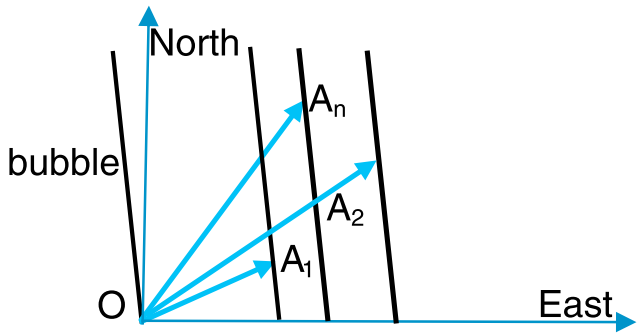

Figure 1. Zonal drift movement of plasma bubble.

2. Method

In this research, only plasma bubbles with obvious scintillations are focused and for its detection, the rate of TEC (total electron content) index (ROTI) is used as an indicator. It is estimated as the standard deviation of rate of TEC (ROT) in a certain time period, typically 5 min, and ROT is given in the unit of TECU/min or so (1 TECU = 10^{16} el/m^2). The threshold value is set to 0.25 TECU [*Nishioka et al.*, 2008]. The time delay is estimated by matching two vertical TEC or slant TEC time series of two GPS stations [*Ji et al.*, 2011].

In order to estimate plasma bubble zonal drift velocity and tilt, for the simplicity of description, the 3-D bubble is imaged as a line with a tilt to the west or east in a plane around 400 km above the Earth, and its mathematical model is

$$kx = y$$

where x and y are the coordinates in the eastward and upward directions and k is the unknown slope related to the tilt. When the bubble is drifting, k will remain the same in short time as the shape of the bubble changes little.

As illustrated in Figure 1, assuming at time t, the bubble intersects at point O (0, 0) with the line between a GPS satellite and a CORS station R. assuming at times t_1, t_2,…, t_n, the bubble intersects at points A_1 (x_1, y_1), A_2 (x_2, y_2),…, A_n (x_n, y_n) with the lines between the GPS satellite and other CORS stations R_1, R_2,…, R_n.

Then, the following equations can be formed:

$$\begin{cases} kx_1 + (v - v_{IPP})(t_1 - t) = y_1 \\ kx_2 + (v - v_{IPP})(t_2 - t) = y_2 \\ \cdots \\ kx_n + (v - v_{IPP})(t_n - t) = y_n \end{cases} . \quad (1)$$

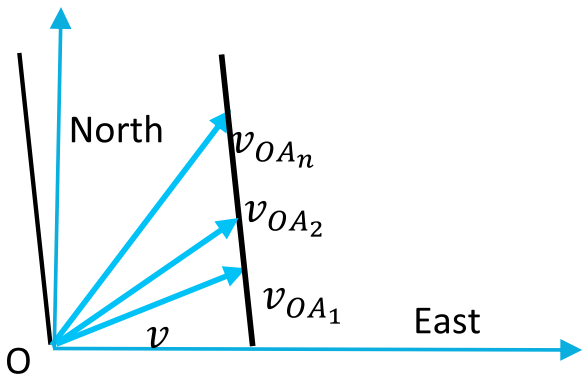

Figure 2. Linear fitting with apparent velocities.

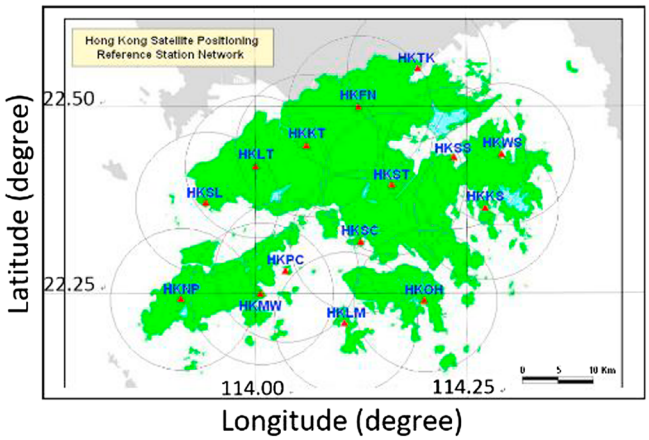

Figure 3. Hong Kong GPS CORS network.

Here v is the zonal drift velocity and v_{IPP} is the zonal velocity of ionospheric pierce point (IPP).

Denoting $A = \begin{bmatrix} x_1 & (t_1 - t) \\ x_2 & (t_2 - t) \\ \cdots & \cdots \\ x_n & (t_n - t) \end{bmatrix}$, $X = \begin{bmatrix} k \\ v \end{bmatrix}$, and $L = \begin{bmatrix} y_1 + v_{IPP}(t_1 - t) \\ y_2 + v_{IPP}(t_2 - t) \\ \cdots \\ y_n + v_{IPP}(t_n - t) \end{bmatrix}$, we will have $AX = L$. With least squares method, k and v can be estimated as $\begin{bmatrix} \hat{k} \\ \hat{v} \end{bmatrix} = (A^T A)^{-1} A^T L$. And, its variance and covariance $\begin{bmatrix} \sigma_k^2 & \sigma_{kv} \\ \sigma_{vk} & \sigma_v^2 \end{bmatrix} = \sigma_0^2 Q$, where $Q = (A^T A)^{-1}$ and $\sigma_0^2 = \frac{V^T V}{n-2}$. Here $V = L - A\hat{X} = L - A\begin{bmatrix} \hat{k} \\ \hat{v} \end{bmatrix}$.

From Figure 2, the apparent velocity can also be estimated. The apparent velocities v_{OA_1}, v_{OA_2},..., and v_{OA_n} along OA_1, OA_2, ..., and OA_n, are equal to $D_{OA_1}/(t_1 - t)$, $D_{OA_2}/(t_2 - t)$, ..., and $D_{OA_n}/(t_n - t)$. If there is no error involved, v_{OA_1}, v_{OA_2}, ..., and v_{OA_n} should be on a line parallel to the bubble as illustrated in Figure 1. So k and v can also be estimated by linear fitting v_{OA_1}, v_{OA_2},..., and v_{OA_n} as shown in Figure 2, which will have the same result from equation (1) theoretically.

3. Numerical Results

Hong Kong is a low-latitude area, around 22.30°N, 114.17°E, dip: 30.5°N (geomagnetic: 11.76°N, 174.75°W; declination: 2.7°W). A local GPS network was developed in 2001 under the charge of Survey and Mapping

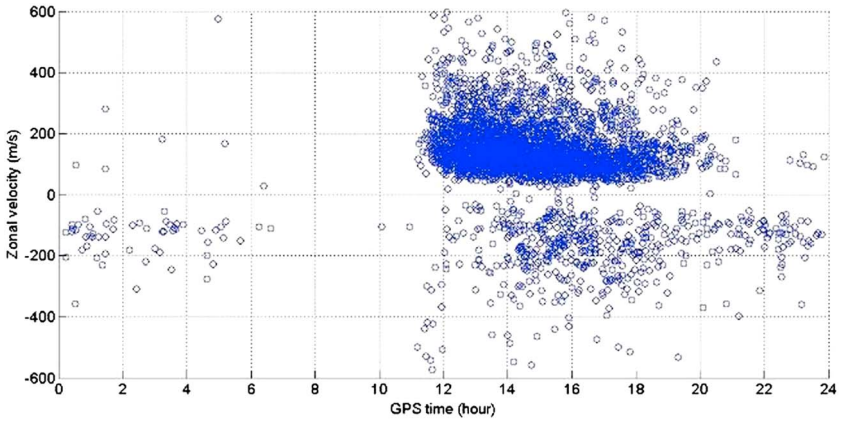

Figure 4. Zonal drift velocity versus GPS time.

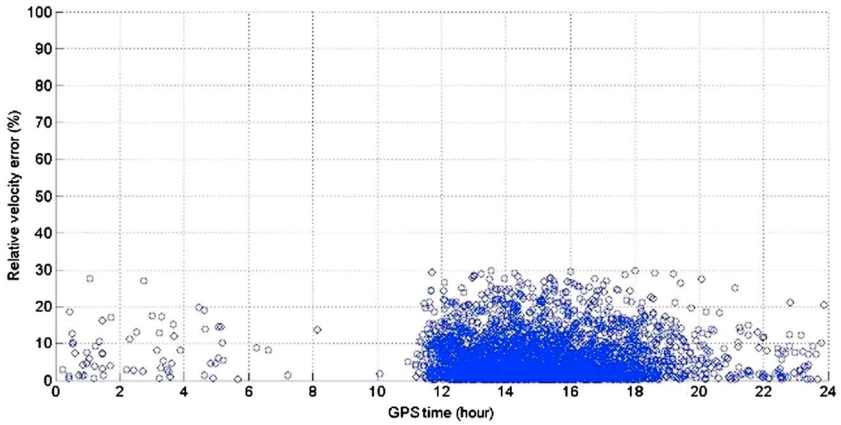

Figure 5. Relative zonal velocity error.

Office of Lands Department, Hong Kong, named as "Hong Kong Satellite Positioning Reference Station Network" (SatRef). Currently, the network consisted of 15 CORS stations evenly distributed in Hong Kong as shown in Figure 3. The GPS observations are collected round-the-clock with a sample interval of 5 s.

In this research, the processed GPS observations for plasma bubble drifting velocity and tilt estimation are collected from 2001 to 2012, covering a whole solar cycle.

With the threshold value of ROTI set to 4 cm (0.25 TECU), a total number of 6146 bubbles have been detected from 2 January 2001 to 31 December 2012. For further statistical analysis, only those with a relative velocity error less than 30% and standard deviation of tilt less than 20° are used and their total number is 3817.

Past research works have shown that the equatorial plasma bubble activity presents a large dependence on the local time, the season, the solar cycle, etc. The diurnal, seasonal, and solar cycle variations of the drift velocity and tilt will be analyzed in detail.

Figure 4 shows the estimated zonal drift velocities versus GPS time (local time = GPS time + about 8 h). From Figure 4, we can see that in nighttime, about 88.6% is eastward and in daytime, about 89.8% is westward. The drift velocity of 74% bubbles is between 50 m/s and 200 m/s. And, in nighttime, whether eastward or westward, the size decreases gradually from around 12:00 to 20:00 GPS time (20:00 to 04:00 local time). Figure 5 gives the relative errors of the estimated velocities, and we can see that most of them are less than 20%.

Figure 6 shows the estimated tilts versus GPS time. Figure 7 gives the standard deviation (SD) of estimated tilts, and we can see that most of them are less than 2°. From Figure 6, we can see that the tilts can be eastward or westward. The inclination of 68.5% cases is between 0° and 20°; that is, most of them are basically vertical within the equatorial plane. But for some of them, the tilt can be as large as more than 60° as

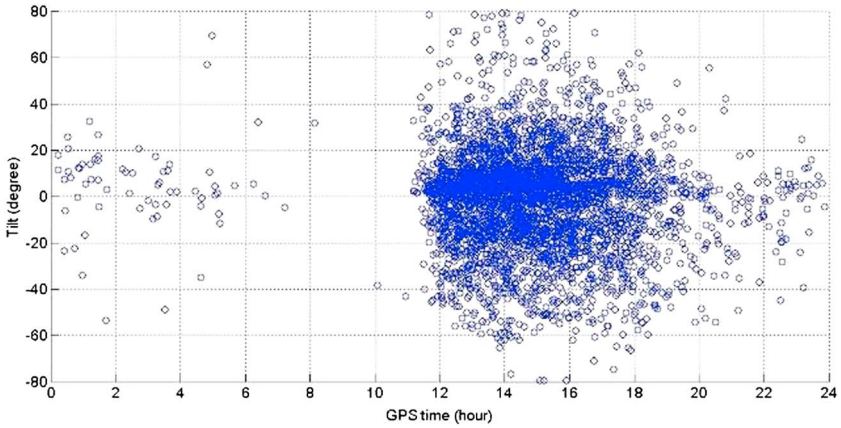

Figure 6. Tilts versus GPS time.

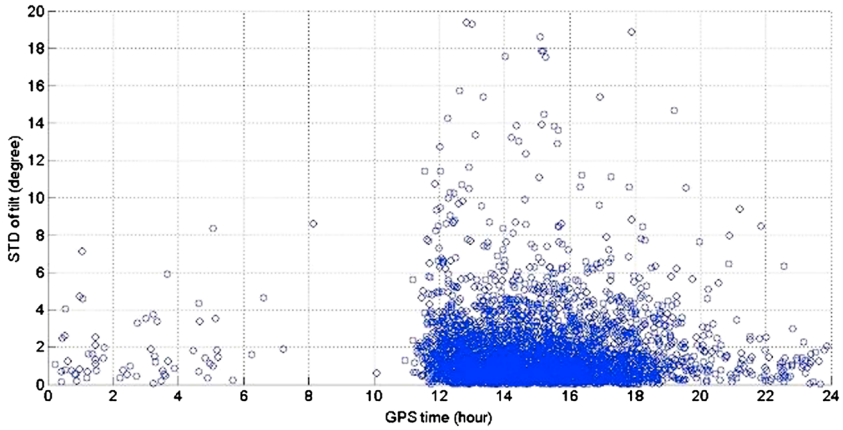

Figure 7. Standard deviation of estimated tilts.

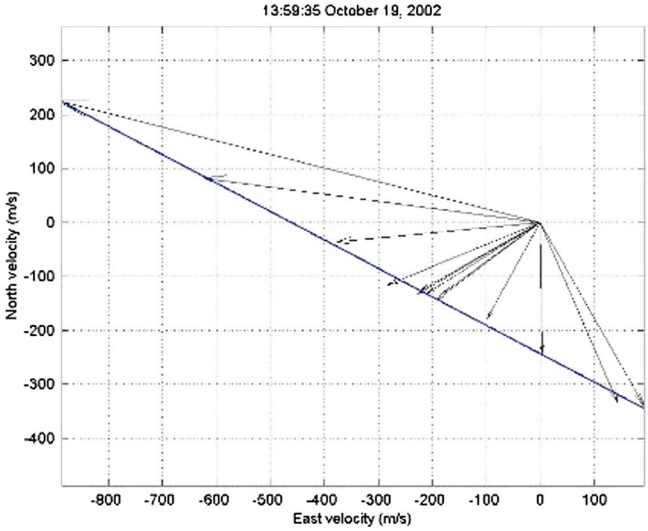

Figure 8. An example of westward tilt of 62°.

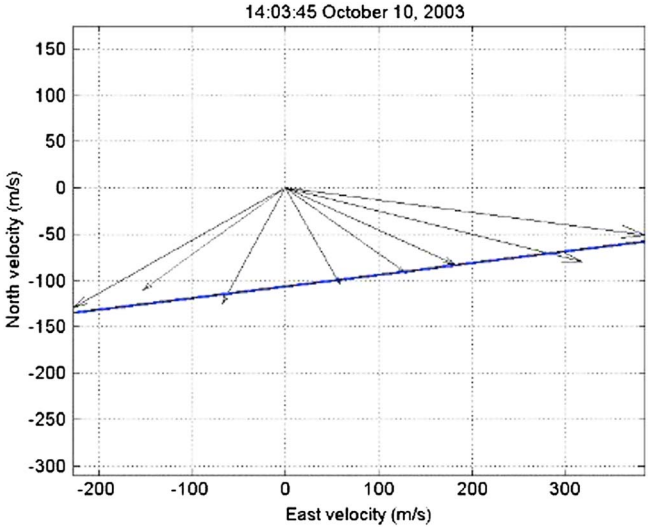

Figure 9. An example of eastward tilt of about 80°.

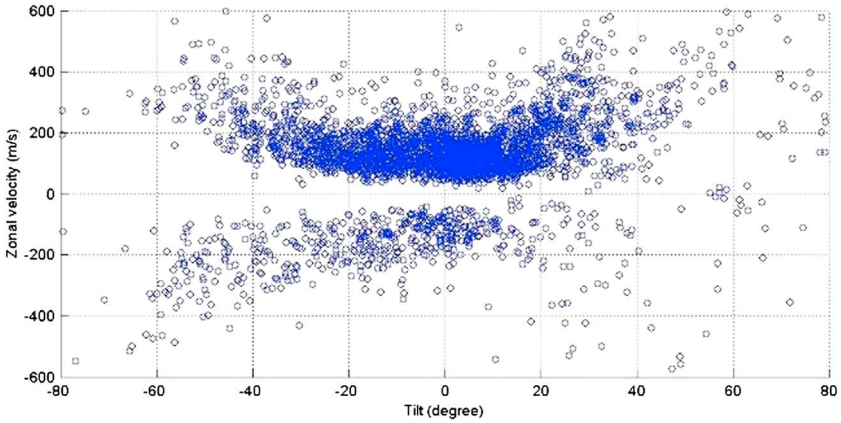

Figure 10. Zonal drift velocities versus tilts.

illustrated in Figure 8 (about 62° with SD of 0.4° (black ones with arrow head are the apparent velocities, and the blue line is the fitting one)), even about 80° as illustrated in Figure 9 (almost 80° with SD of 0.3°).

Figure 10 shows the estimated zonal drift velocities versus tilts. It looks that they are correlated. When the zonal drift velocity increases (>200 m/s), the tilt also increases (>20°or even 40°). If only taking the data of the upper part of Figure 10 into consideration (velocity > 0), the regression coefficients are 136.72, 0.36, and 0.06 and the estimated quadratic regression function is velocity = 136.72 + 0.36 tilt + 0.06 $tilt^2$ with no less than 95% confidence level of *F* test.

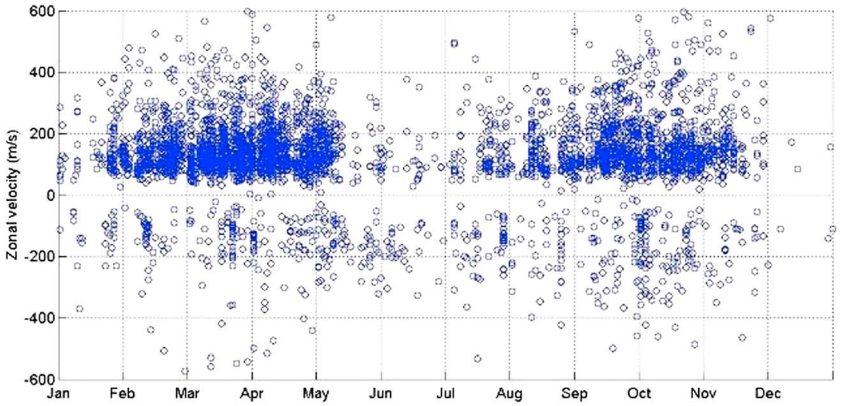

Figure 11. Seasonal zonal velocity distribution.

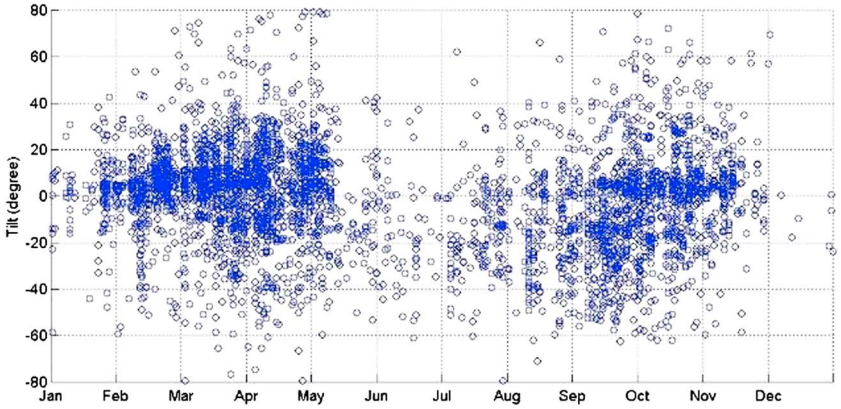

Figure 12. Seasonal tilt distribution.

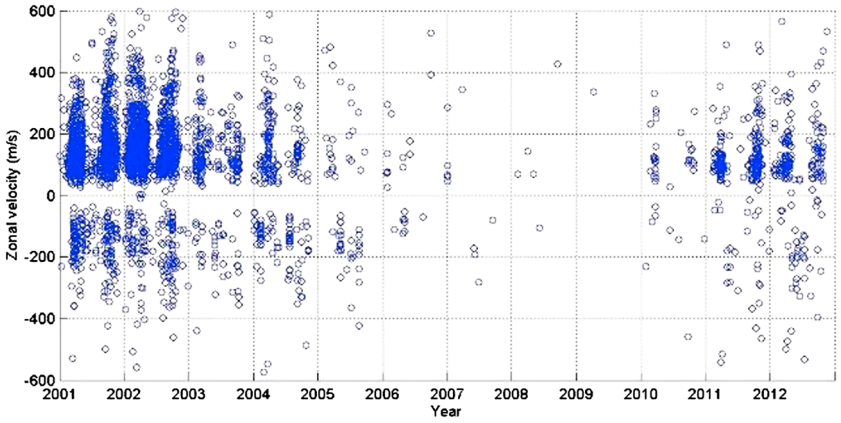

Figure 13. Yearly zonal velocity distribution.

Figures 11 and 12 show the seasonal zonal velocity and tilt distribution. It looks that the zonal drift velocities and tilts with large values (>400 m/s or >40°) generally occur in spring and autumn.

Figures 13 and 14 show the yearly zonal velocity and tilt distribution. It looks that the zonal drift velocity and tilt with big size (>400 m/s or >40°) generally occur in solar active years, such as 2001, 2002, 2003, and 2012.

4. Summary and Discussion

It had been established that the equatorial plasma bubble activity occurs mainly during the nighttime and a bubble typically forms following sunset, drifts eastward, and the eastward drifting velocity decreases gradually, then turns to west steadily after midnight. A gradual decrease in the zonal drift velocity from between 100 and 200 m/s at around 22:00 LT to below 50 m/s after local midnight was reported [*Mendillo and Baumgardner*, 1982; *Mendillo et al.*, 1997; *Taylor et al.*, 1997; *Sinha and Raizada*, 2000; *Pimenta et al.*, 2003].

In general agreement with other works, the present results indicate that the equatorial plasma bubble activity is predominantly a nighttime phenomenon. From Figure 4, we can see that the drift generally starts from around 12:00 GPS time (20:00 local time) after sunset with an average velocity of 160 m/s eastward decreases gradually and ends around 20:00 GPS time (04:00 local time). But different from the typical pattern, most of the cases do not turn westward and the velocity is generally not less than 50 m/s even after midnight. There are also cases with westward drift just after sunset.

About the seasonal characteristics, past research works showed the seasonal dependence of the equatorial plasma bubble activity [*Makela et al.*, 2004]. Most of the seasonal maxima are from February to April and from September to November. Although generally around one or both equinoxes, the maxima are not the exactly

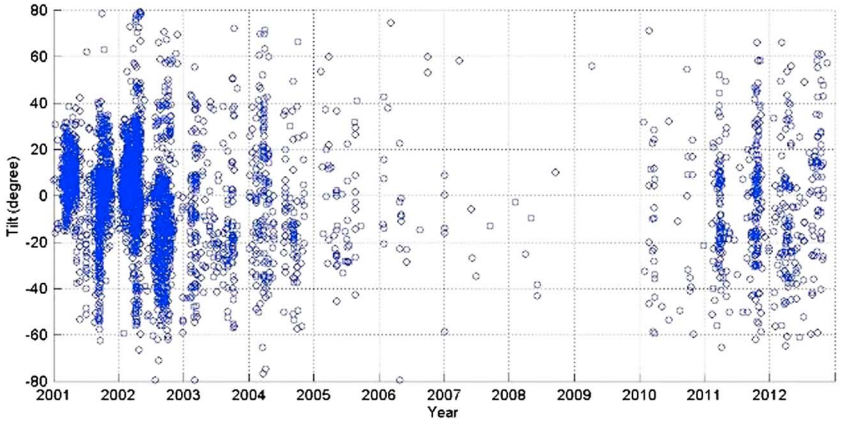

Figure 14. Yearly tilt distribution.

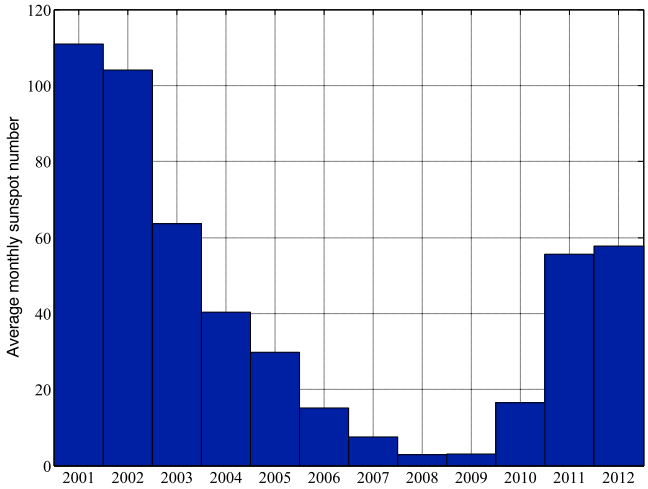

Figure 15. Average monthly sunspot number from 2001 to 2012.

same and can be different with different year, frequency, and longitude. And, also the asymmetry between equinoxes is not rare.

From Figure 11, we can see that present results are basically consistent with past research works. The drift maxima are from February to May and from August to November. During these two periods, the occurrence rate is much higher and the drift velocity is also higher than the other time.

The equatorial plasma bubble activity is dependent on the solar cycle, which is the periodic change in the Sun's activity and can be represented by the number of sunspots. The solar cycle has an average duration of about 11 years, and the last maximum was in 2001—the starting date of our GPS observations. Past research found that the occurrence of equatorial plasma bubbles is closely related to the number of sunspots and it is obviously a consequence of the solar activity [*Sobral and Abdu*, 1991].

Figure 15 shows the average monthly sunspot number from 2001 to 2012. Comparing with Figures 13 and 14, we can see that the average monthly sunspot number is consistent with the occurrence of plasma bubble, the drift velocity, and tilt. With larger sunspot numbers in 2001, 2002, 2003, 2011, and 2012, the occurrence rates are also higher in these years and larger drift velocity (>200 m/s) and tilt (>20°) also occurred in these years. The present results agree well to the past research works.

5. Conclusions

In this research, first, an estimation method for zonal drift velocity and tilt of equatorial plasma bubble is proposed based on GPS CORS network. And, a detailed study and analysis are made on characteristics of zonal drift velocity and tilt based on the observations of Hong Kong GPS CORS network from 2001 to 2012, covering a whole solar cycle period.

Based on the results, the following conclusions can be drawn:

1. Generally, the drift velocity is eastward in nighttime. The size is between 50 m/s and 200 m/s and decreases gradually from around 20:00 local time to 03:00 next morning.
2. Generally, the tilt is less than 20°in nighttime and can be eastward and westward.
3. It looks that drift velocity and tilt are correlated. When drift velocity is big, the corresponding tilt is also big.
4. It looks that big drift velocity and tilt occur generally in spring and autumn and in solar active years.

Acknowledgments

The data for this paper can be downloaded from the homepage of Surveying and Mapping Office, Lands Department, Hong Kong: http://www.geodetic.gov.hk/smo/gsi/programs/en/GSS/satref/satref.htm. The research was substantially funded by Hong Kong Research Grants Council Competitive Earmarked Research Grant (PolyU 152023/14E), the research fund from the Research Institute of Sustainable Urban Development, Hong Kong Polytechnic University, the Fundamental Research Funds for the Central Universities (grants 14CX02036A, 14CX02033A, 14CX02039A, and 11CX05015A), National Natural Science Foundation of China (grants 41374008, 41274006, 41274011, and 41001250), and Natural Science Foundation of Shandong Province, China (grants ZR2012DM010 and ZR2011DQ011).

Alan Rodger thanks Rajkumar Hajra and another reviewer for their assistance in evaluating this paper.

References

Aarons, J. (1993), The longitudinal morphology of equatorial F-layer irregularities relevant to their occurrence, *Space Sci. Rev.*, *63*, 209–243.

Aarons J., M. Mendillo and R. Yantosca (1996), GPS phase fluctuations in the equatorial region, Proceedings of the 1996 Ionospheric Effects Symposium, Alexandria, Va.

Abalde, J., P. Fagundes, J. Bittencourt, and Y. Sahai (2001), Observations of equatorial F region plasma bubbles using simultaneous OI 777.4 nm and OI 630.0 nm imaging: New results, *J. Geophys. Res.*, *106*, 30,331–30,336, doi:10.1029/2001JA001115.

Abdu, M., J. Sobral, Y. Nakamura, and C. Zamlutti (1987), Equatorial plasma bubble zonal velocity height gradient from spaced VHF polarimeter and scanning 630 nm measurements, *J. Geophys. Res.*, *14*, 965–968.
Aggson, T., N. Maynard, F. Herrero, H. Mayr, L. Brace, and M. Liebrecht (1987), Geomagnetic equatorial anomaly in zonal plasma-flow, *J. Geophys. Res.*, *92*, 311–315, doi:10.1029/JA092iA01p00311.
Basu, S., et al. (1996), Scintillations, plasma drifts, and neutral winds in the equatorial ionosphere after sunset, *J. Geophys. Res.*, *101*, 26,795–26,809, doi:10.1029/96JA00760.
Beach, T., M. Kelley, P. Kintner, and C. Miller (1997), Total electron content variations due to nonclassical traveling ionospheric disturbances: Theory and global positioning system observations, *J. Geophys. Res.*, *102*, 7279–7292, doi:10.1029/96JA02542.
Coley, W., and R. Heelis (1989), Low-latitude zonal and vertical ion drifts seen by DE 2, *J. Geophys. Res.*, *94*, 6751–6761, doi:10.1029/JA094iA06p06751.
Fejer, B. (1981), The equatorial ionospheric electric field: A review, *J. Atmos. Terr. Phys.*, *43*, 377–386.
Fejer, B., E. de Paula, S. Gonzalez, and R. Woodman (1991), Average vertical and zonal F-region plasma drifts over Jicamarca, *J. Geophys. Res.*, *96*, 13,901–13,906, doi:10.1029/91JA01171.
Fejer, B., R. Heelis, and W. Hanson (1995), Global equatorial ionospheric vertical plasma drifts measured by the AE-E satellite, *J. Geophys. Res.*, *100*, 5769–5776, doi:10.1029/94JA03240.
Ji, S., W. Chen, X. Ding, and C. Zhao (2011), Equatorial ionospheric zonal drift by monitoring local GPS reference networks, *J. Geophys. Res.*, *116*, A08310, doi:10.1029/2010JA015993.
Kelley, M., D. Kotsikopoulos, T. Beach, D. Hysell, and S. Musman (1996), Simultaneous Global Positioning System and radar observations of equatorial spread F at Kwajalein, *J. Geophys. Res.*, *101*, 2333–2341, doi:10.1029/95JA02025.
Kil, H., P. Kintner, E. R. de Paula, and E. Kantor (2000), Global positioning system measurements of the ionospheric zonal apparent velocity at Cachoeira Paulista in Brazil, *J. Geophys. Res.*, *105*, 5317–5327, doi:10.1029/1999JA000244.
Kil, H., P. M. Kintner, E. de Paula, and I. Kantor (2002), Latitudinal variations of scintillation activity and zonal plasma drifts in South America, *Radio Sci.*, *37*(1), 1006, doi:10.1029/2001RS002468.
Kintner, P., H. Kil, T. Beach, and E. R. de Paula (2001), Fading timescales associated with GPS signals and potential consequences, *Radio Sci.*, *36*, 731–743, doi:10.1029/1999RS002310.
Kintner, P. M., B. M. Ledvina, E. R. de Paula, and I. J. Kantor (2004), Size, shape, orientation, speed, and duration of GPS equatorial anomaly scintillations, *Radio Sci.*, *39*, RS2012, doi:10.1029/2003RS002878.
Makela, J., and M. Kelley (2003), Field-aligned 777.4 nm composite airglow images of equatorial plasma depletions, *Geophys. Res. Lett.*, *30*(8), 1442, doi:10.1029/2003GL017106.
Makela, J., B. Ledvina, M. Kelley, and P. Kintner (2004), Analysis of the seasonal variations of equatorial plasma bubble occurrence observed from Haleakala, Hawaii, *Ann. Geophys.*, *22*, 3109–3121.
Martinis, C., J. Eccles, J. Baumgardner, J. Manzano, and M. Mendillo (2003), Latitude dependence of zonal plasma drifts obtained from dual-site airglow observations, *J. Geophys. Res.*, *108*(A3), 1129, doi:10.1029/2002JA009462.
Mendillo, M., and J. Baumgardner (1982), Airglow characteristics of equatorial plasma depletions, *J. Geophys. Res.*, *87*, 7641–7652, doi:10.1029/JA087iA09p07641.
Mendillo, M., and A. Tyler (1983), Geometry of depleted plasma regions in the equatorial ionosphere, *J. Geophys. Res.*, *88*, 5778–5782, doi:10.1029/JA088iA07p05778.
Mendillo, M., J. Baumgardner, M. Colerico, and D. Nottingham (1997), Imaging science contributions to equatorial aeronomy: Initial results from the MISETA program, *J. Atmos. Terr. Phys.*, *59*(13), 1587–1599.
Mukherjee, G. (2003), Studies of the equatorial F-region depletions and dynamics using multiple wavelength nightglow imaging, *J. Atmos. Terr. Phys.*, *65*(3), 379–390.
Musman, S., J. Jahn, J. LaBelle, and W. Swartz (1997), Imaging spread-F structures using GPS observations at Alcântara, Brazil, *Geophys. Res. Lett.*, *24*, 1703–1706.
Nishioka, M., A. Saito, and T. Tsugawa (2008), Occurrence characteristics of plasma bubble derived from global ground-based GPS receiver networks, *J. Geophys. Res.*, *113*, A05301, doi:10.1029/2007JA012605.
Ogawa, T., E. Sagawa, Y. Otsuka, K. Shiokawa, T. Immel, S. Mende, and P. Wilkinson (2005), Simultaneous ground- and satellite-based airglow observations of geomagnetic conjugate plasma bubbles in the equatorial anomaly, *Earth Planets Space*, *57*, 385–392.
Ogawa, T., Y. Otsuka, and K. Shiokaw (2006), Ionospheric disturbances over Indonesia and their possible association with atmospheric gravity waves from the troposphere, *J. Meteorol. Soc. Jpn.*, *84A*, 327–342.
Otsuka, Y., K. Shiokawa, and T. Ogawa (2006), Equatorial ionospheric scintillations and zonal irregularity drifts observed with closely-spaced GPS receivers in Indonesia, *J. Meteorol. Soc. Jpn.*, *84A*, 343–351.
Pimenta, A., P. Fagundes, Y. Sahai, J. Bittencourt, and J. Abalde (2003), Equatorial F-region plasma depletion drifts: Latitudinal and seasonal variations, *Ann. Geophys.*, *21*(12), 2315–2322.
Rohrbaugh, R., W. Hanson, B. Tinsley, B. Cragin, and J. McClure (1989), Images of transequatorial bubbles based on field-aligned airglow observations from Haleakela in 1984–1986, *J. Geophys. Res.*, *94*, 6763–6770, doi:10.1029/JA094iA06p06763.
Sinha, H., and S. Raizada (2000), Some new features of ionospheric plasma depletions over the Indian zone using all sky optical imaging, *Earth Planets Space*, *52*(8), 549–559.
Sobral, J., and M. Abdu (1990), Latitudinal gradient in the plasma bubble zonal velocities as observed by scanning 630 nm airglow measurements, *J. Geophys. Res.*, *95*, 8253–8257, doi:10.1029/JA095iA06p08253.
Sobral, J., and M. Abdu (1991), Solar activity effects on equatorial plasma bubble zonal velocity and its latitude gradient as measured by airglow scanning photometers, *J. Atmos. Terr. Phys.*, *53*, 729–742.
Sobral, J., M. Abdu, H. Takahashi, H. Sawant, C. Zamlutti, and G. Borba (1999), Solar and geomagnetic activity effects on nocturnal zonal drifts of ionospheric plasma depletions, *Adv. Space Res.*, *24*(11), 1507–1510.
Taylor, M., J. Eccles, J. LaBelle, and J. Sobral (1997), High resolution OI (630 nm) image measurements of F-region depletion drifts during the Guará Campaign, *Geophys. Res. Lett.*, *24*, 1699–1702, doi:10.1029/97GL01207.
Taylor, M., P. Pautet, A. Medeiros, R. Buriti, J. Fechine, D. Fritts, S. Vadas, H. Takahashi, and F. São Sabbas (2009), Characteristics of mesospheric gravity waves near the magnetic equator, Brazil, during the SpreadFEx campaign, *Ann. Geophys.*, *27*, 461–472.
Tinsley, B., P. Rohrbaugn, W. Hanson, and A. Broadfoot (1997), Images of transequatorial F region bubbles in 630- and 777-nm emissions compared with satellite measurements, *J. Geophys. Res.*, *102*, 2057–2077.